


ORIGINAL ARTICLE

Carbofuran accelerates the cellular senescence and declines the life span of *spns1* mutant zebrafish

Alam Khan^{1,2}  | Talukdar Mohammad Fahad¹ | Tanjima Akther¹ | Tanjeena Zaman^{3,4} | Md Faruk Hasan⁵ | Md Rafiqul Islam Khan¹ | Mohammad Saiful Islam¹ | Shuji Kishi⁶

¹Department of Pharmacy, University of Rajshahi, Rajshahi, Bangladesh

²Department of Molecular Medicine, The Scripps Research Institute, Jupiter, FL, USA

³Department of Fisheries, University of Rajshahi, Rajshahi, Bangladesh

⁴Department of Biology, University of Hail, Hail, Saudi Arabia

⁵Department of Genetic Engineering and Biotechnology, University of Rajshahi, Rajshahi, Bangladesh

⁶S&J Kishi Research Corporation, Jupiter, FL, USA

Correspondence

Alam Khan, Department of Pharmacy, University of Rajshahi, Rajshahi-6205, Bangladesh.
Emails: alamkhan792002@yahoo.co.in; alamkhan@ru.ac.bd

Funding information

Ministry of Science and Technology Special Allocation Research Fund, Grant/Award Number: 39.00.0000.009.06.024.19-665/460-ID; Rajshahi University Research grant, Grant/Award Number: A1386/5/52/RU/Science-24/18-19; The World Academy of Sciences, Grant/Award Number: 17-414 RG/BIO/AS_I - FR3240297760

Abstract

Carbofuran is a carbamate pesticide, widely used in agricultural practices to increase crop productivity. In mammals, carbofuran is known to cause several untoward effects, such as apoptosis in the hippocampal neuron, oxidative stress, loss of memory and chromosomal anomalies. Most of these effects are implicated with cellular senescence. Therefore, the present study aimed to determine the effect of carbofuran on cellular senescence and biological ageing. Spinster homolog 1 (*Spns1*) is a transmembrane transporter, regulates autolysosomal biogenesis and plays a role in cellular senescence and survival. Using senescence-associated β -galactosidase staining, we found that carbofuran accelerates the cellular senescence in *spns1* mutant zebrafish. The yolk opacity, a premature ageing phenotype in zebrafish embryos, was accelerated by carbofuran treatment. In the survival study, carbofuran shortened the life span of *spns1* mutant zebrafish. Autophagy is the cellular lysosomal degradation, usually up-regulated in the senescent cells. To know the impact of carbofuran exposure on autophagy progress, we established a double-transgenic zebrafish line, harbouring EGFP-tagged LC3-II and mCherry-tagged Lamp1 on *spns1* mutant background, whereas we found, carbofuran exposure synergistically accelerates autolysosome formation with insufficient lysosome-mediated degradation. Our data collectively suggest that carbofuran exposure synergistically accelerates the cellular senescence and affects biological ageing in *spns1* defective animals.

KEYWORDS

carbofuran, life span, senescence, spinster homolog 1, zebrafish

1 | INTRODUCTION

Senescence is a cellular process that implements permanent cell cycle arrest in response to various stimuli, such as oxidative stress, telomere loss, chemotherapeutic drugs, DNA damage and oncogenic signalling.^{1,2} The elevated intensity of senescent cells mainly

exists in ageing tissues, because of its implication with ageing.¹ Ablation of senescent cells by mechanical or other means improve health outcome as well as prolongs biological ageing.³ Activation of senescence-associated beta-galactosidase (SA- β -gal) in the senescent cell is considered as the hallmark of cellular senescence.^{4,5} Although the maximum beta-galactosidase activity can be seen at

This is an open access article under the terms of the Creative Commons Attribution License, which permits use, distribution and reproduction in any medium, provided the original work is properly cited.

© 2020 The Authors. *Journal of Cellular and Molecular Medicine* published by Foundation for Cellular and Molecular Medicine and John Wiley & Sons Ltd

medium to strong acidic pH, the least activity that can be found at pH 6, which typically uses to examine the senescent and ageing cells.⁶ On the other hand, autophagy is a cellular lysosomal degradation process, essential to regulate energy homeostasis through recycling unnecessary or dysfunctional cytoplasmic constituents.⁷ In normal cells, autophagy occurs at low baseline altitudes, which is elevated in the senescent cells.⁸ Autophagy is initiated with the formation of the phagophore from a variety of sources, such as ER-mitochondrial junctions, ER-plasma membrane contact sites and ER-Golgi intermediate compartment. Then, phagophore wraps unnecessary or dysfunctional cytoplasmic constituents to build-up autophagosomes, which successively fuse with lysosomes to form autolysosomes.^{9,10} Finally, through the utilization of lysosomal hydrolases, the contents of autophagosomes are degraded and recycled. The vacuolar H⁺-ATPase (V-ATPase) is a proton pump, which establishes and sustains an acidic condition within the lysosome. The V-ATPase promotes autophagosome-lysosome fusion and lysosome-mediated degradation of the contents of autophagosomes.¹¹

Lysosomal degradation yields are released into the cytosol through the lysosomal efflux transporter system. Spinster homolog 1 (Spns1) in vertebrates is known as Spinster (Spin) in flies, encodes a putative lysosomal efflux permease, whose amino acid sequence has resembled the amino acid sequence of lysosomal sugar carrier.¹² The spin mutation is associated with neurodegeneration, rejection behaviour against the opposite sex and shortened life span in flies.¹³ In zebrafish, the loss of *spns1* gene leads to the accumulation of opaque substances in the yolk, and yolk extension and reduces biological ageing.^{12,14} Recently, we found that the concurrent disruption of the V-ATPase subunit gene, *ATPase*, *H⁺ transporting, lysosomal, VO subunit Ca (atp6v0ca)* in *spns1* mutant fish synergistically induced cellular senescence and shorten the life span.¹⁵

Carbofuran is a toxic carbamate pesticide, whose chemical name is 2,3-dihydro-2,2-dimethyl-7-benzofuranyl methylcarbamate.¹⁶ It is widely used to control pests in agricultural fields, particularly in developing countries.^{17,18} It has insecticidal, nematocidal and acaricidal activities.^{19,20} In Bangladesh, 37% of the total sold pesticides during 2007 was carbofuran.²¹ Humans, particularly in agricultural dependent countries, are often exposed to pesticides including carbofuran through contaminated water, air and vegetables.^{22,23} The World Health Organization (WHO) classified carbofuran as a highly hazardous pesticide (category 1b).²⁴ Its toxicity to mammals leads to sperm abnormalities and chromosomal aberrations.²³ Carbofuran suppresses anti-oxidative enzymes in the body, such as glutathione-S-transferase and superoxide dismutase, and induces oxidative stress through the generation of reactive oxygen species (ROS).^{25,26} It causes apoptosis of hippocampal neurons through inducing DNA fragmentation,²⁷ also causes Alzheimer's syndrome type pathology in the central nervous system.²⁸ Furthermore, carbofuran reduces ATP generation in neurons through the inhibition of glycolysis and Krebs's cycle.^{29,30}

The detrimental effects of carbofuran on the anti-oxidative defence system as well as on the nervous system suggest its implication in cellular senescence and biological ageing. However, the role of carbofuran on cellular senescence and/or biological ageing still remains obscure. In the present study, we found that carbofuran synergistically accelerates the cellular senescence and shortens the life span of *spns1* mutant zebrafish. In addition, using a transgenic zebrafish line [Tg(EGFP-LC3); *spns1*^{+/−}], expressing EGFP-tagged microtubule-associated protein 1 light chain 3-II (LC3-II) on autophagosome, it was revealed that carbofuran affects the autophagy process in *spns1* mutant fish.

2 | MATERIALS AND METHODS

2.1 | Chemicals and reagents

Carbofuran of analytical grade was procured from Merck, Germany (SKU 32056). Its stock solution was prepared by solubilizing in DMSO, which was diluted in egg water to prepare the final solution for treatment. The solution to be used for the control group was prepared likely by diluting an equal volume of DMSO in egg water. Reagents such as potassium ferrocyanide, potassium ferricyanide, 1-phenyl-2-thiourea, paraformaldehyde and MgCl₂ were purchased from Sigma-Aldrich, Germany (SKU P3289, 702587, P7629, 16005 and M8266).

2.2 | Zebrafish husbandry

Adult zebrafish of both wild and mutant types were harboured under a 14-hour light/10-hour dark cycle at 25°C. Zebrafish embryos were maintained and raised at 28.5°C under the same light-dark cycle. After three weeks of embryonic development, all embryos were maintained under adult fish condition. Zebrafish were fed with both brine shrimp and flake food, each once daily. Using a circulation system, water of zebrafish tanks were replaced at each 10-15 minutes interval. Hours of post-fertilization (hpf) of Kimmel et al³¹ was considered to determine the developmental stages of embryos.

2.3 | Generation of transgenic zebrafish

PT2-EGFP-LC3 and PT2-mCherry-Lamp1 plasmids were kindly donated by Dr Shuji Kishi Lab of the Scripps Research Institute, Florida, USA. Tol2 transposase mRNA was synthesized using SP6 RNA polymerase kit (Ambion, AM1340). Collected plasmids concurrently with Tol2 transposase mRNA were microinjected into embryos of the one-cell stage. Embryos having significant green and/or red fluorescent expression under the fluorescence condition of the microscope were sorted, raised to adulthood and mated with wild fishes to

find germline-transmitted embryos. Embryos having a green or red fluorescent expression of nearly similar intensity were founder zebrafish (F0) embryos, which were raised to adulthood and incrossed to give F1 generation as described.³² Adult F1 fishes were mated, and resulting embryos were used in experiments.

2.4 | Senescence-associated β -galactosidase activity assay

Embryonic senescence caused by chemical-induced oxidative stress and gene mutation can be detected using the SA- β -gal assay.³³ A chemical reagent, 5-bromo-4-chloro-3-indolyl β -D-galactopyranoside, is widely used for SA- β -galactosidase staining, and their interactions are signposted by blue staining. Embryos were washed with phosphate buffer saline (PBS) solution and fixed in 4% paraformaldehyde. After around 12 hours of fixation, embryos were washed three times with PBS solution and two times with staining buffer. The staining buffer was prepared by dissolving potassium ferricyanide (5 mmol/L), potassium ferrocyanide (5 mmol/L) and MgCl_2 (2 mmol/L) in PBS solution, where the pH of the solution was adjusted around 6.0 using NaOH and/HCl. Staining was conducted by immersing embryos in the staining buffer, which containing 5-bromo-4-chloro-3-indolyl β -D-galactopyranoside (X-gal) at the concentration of 20 $\mu\text{g}/\text{ml}$. The embryonic preparation was kept at 10°C until sufficient staining. Then, embryos were re-washed four times with PBS solution and photographed. The staining intensity of the captured images was quantified using Adobe Photoshop CS software.¹⁴

2.5 | Chemical treatments

Zebrafish embryos were treated at a number of late developmental stages. All treatments were performed with a six-well plate. Based on the literature survey, several concentrations of carbofuran (10, 100 and 200 $\mu\text{mol}/\text{L}$) were prepared to select the maximum effective concentration (without inducing toxic morphological abnormality). The maximum effect (SA- β -gal activity) was found at 100 $\mu\text{mol}/\text{L}$ concentration of carbofuran (Figure 2B), and the concentration did not significantly affect the morphological phenotype of embryos. The higher concentration of carbofuran (200 $\mu\text{mol}/\text{L}$) was excluded from subsequent experiments because of its shortening effect on the body length of zebrafish embryos (data have not shown). The applied carbofuran solution was replaced by a fresh carbofuran solution at each 12 hours interval. Treated embryos were maintained at 28.5°C, under 14-hour light/10-hour dark cycle. During treatment, embryos were observed under a microscope at each 3 hours interval. All abnormalities or deaths observed were recorded, and dead embryos were removed from the treatment solution. All experiments were approved by the Institutional Animal, Medical Ethics, Biosafety, and Biosecurity Committee of the Institute of Biological Science (I. B.

Sc.) of the University of Rajshahi, Bangladesh (245/451/IAMEBBC/IBSc). The guidelines of I. B. Sc. were followed in animal handling.

2.6 | Heterozygote $spns1^{+/\text{hi891}}$ fish identification

Heterozygote $spns1^{+/\text{hi891}}$ (hereafter $spns1^{+/-}$) fish was kindly donated by Dr Shuji Kishi Lab of the Scripps Research Institute, Florida, USA. To identify heterozygote $spns1^{+/-}$ fishes, DNA was extracted from the tail fin of zebrafish, and then, genomic and mutant sequences of heterozygote $spns1^{+/-}$ fishes were amplified using PCR reactions. The primers used are $spns1$ genomic forward (5'-AGGTAAAGACAGCCCCGAAAC-3'), $spns1$ genomic reverse (5'-GATCCCAGACGCCAACATTA-3'), $spns1$ (*hi891*) mutant forward (5'-TAAGTCGGTTCGGCTGCACGGTT-3'), and $spns1$ (*hi891*) mutant reverse (5'-TGATCTCGAGTTCCTTGGGAGGGTCT-3'). Wild fish ($spns1^{+/+}$) harbouring only $spns1$ genomic sequence, whereas heterozygote fish ($spns1^{+/-}$) harbouring both $spns1$ genomic and $spns1$ (*hi891*) mutant sequences, and homozygote $spns1^{\text{hi891}/\text{hi891}}$ fish (hereafter $spns1^{-/-}$) has only $spns1$ (*hi891*) mutant sequence.³⁴

2.7 | Lysosomal staining

At the beginning of the autophagy process, microtubule-associated protein 1 light chain 3-II (LC3II, hereafter mentioned as LC3) is formed at the inner membrane of the autophagosome.^{15,35} Transgenic zebrafish expressing EGFP-LC3 on $spns1^{+/-}$ heterozygote background [Tg(EGFP-LC3); $spns1^{+/-}$] was used to estimate the progress in autophagy. Although autophagy keeps in progress, autophagosomes are fuses with the lysosomes to form autolysosomes, where the content of autophagosomes is sequestered by the lysosomal enzymes.^{32,36} To estimate the co-localization of the autophagosome with the lysosome, LysoTracker Red DND-99 (Invitrogen/Molecular Probes, L7528) was used to stain the lysosome. Staining was carried out by incubating embryos at 28.5°C for 1 hour in PBS solution, which containing LysoTracker Red DND-99 at the concentration of 0.005 $\mu\text{mol}/\text{L}$.

2.8 | Microscopy and imaging

Imaging was carried out using both macrofluorescence microscope (Nikon AZ100) and confocal microscope (Olympus; FluoView 1000). Before live imaging, embryos were anaesthetized with tricaine solution (0.16 mg/ml). The whole body of SA- β -gal stained fish was photographed using the reflected bright light of the Nikon AZ100 microscope. In addition, the cellular SA- β -gal staining signal was observed under the confocal microscope. In each experiment, all images were taken under the same condition of the microscope.

TABLE 1 List of primers used for RT-PCR analysis

Genes	Primers	Annealing temp (°C)	Cycles
<i>pai-1</i>	Forward: CTGATCTTTGCCCTTTGCGCATCA Reverse: TTTGCTCAAGCTGCGCTAAAGAC	55	25
<i>p21</i>	Forward: TGAGAACTTACTGGCAGCTTCA Reverse: ACGTGCATTCTGCTCGTAGC	55	25
<i>smp-30</i>	Forward: ACTATGACATCCAAACTGGAGGA Reverse: CTTCTGTGTCTATGCACATACCG	51	25
β -actin	Forward: CCCAGACATCAGGGAGTGAT Reverse: CACCGATCCAGACGGAGTAT	60	18

Note: During PCR amplification, the initial denaturing was carried out at 94°C for 5 min. Amplicon size (bp) of RT-PCR products were 354, 396, 98 and 896 for *pai-1*, *p21*, *smp30* and β -actin, respectively.

2.9 | RT-PCR analysis

Regulations of mRNA levels of *pai1*, *p21* and *smp30* genes were estimated by RT-PCR analysis. Total RNA was isolated using TRIzol reagent (Invitrogen, 15596026), and double-strand cDNA was synthesized using M-MLV reverse transcriptase (Promega, M1705). RT-PCR primers sequences were presented in Table 1 including their annealing temperatures and amplification cycle.

2.10 | Quantitative analysis

Intensities of fluorescence of captured images were quantified using Adobe Photoshop CS software. PCR bands were quantified by ImageJ software (Java-based image processing program developed by NIH). Data analysis was carried out using SPSS statistics software (version 15.0). Data are presented as mean \pm SEM. A comparison among different groups was made by Student's *t* test.

3 | RESULTS

3.1 | Carbofuran synergistically accelerates the senescence-associated- β -galactosidase activity in *spns1*^{-/-} mutant zebrafish

When heterozygote *spns1*^{+/-} adult fishes were incrossed, around 25% of resultant embryos have shown homozygous (*spns1*^{-/-}) phenotypes (Figure 1A). The most prominent morphological phenotype in homozygous embryos was yolk opaqueness. Although homozygous fishes had a short life span (4-6 days), heterozygous fishes developed into adulthood normally without any yolk opaqueness phenotype.^{14,34} Increased SA- β -gal activity because of the senescence induction was established in *spns1*^{-/-} mutant fish.^{12,14} We confirmed both the yolk opaqueness phenotype and the up-regulation of SA- β -gal activity in our homozygous fishes (Figure 1B,C). Besides, a much stronger yolk opaqueness phenotype was found in carbofuran treated homozygous (*spns1*^{-/-}) fish (Figure 1B). The SA- β -gal staining intensity throughout the whole body of fish was examined under a

stereo-microscope (macromicroscopy). In addition, blue particles of SA- β -gal staining at the cellular level around the head region (dorsal to the eye) were determined by a confocal microscopic examination. Carbofuran treatment accelerated SA- β -gal activity under both microscopic observations (Figure 1D,E). Macromicroscopic observation particularly indicated an enhancement of SA- β -gal staining intensity at the head and tail regions (Figure 1C), whereas the carbofuran treated group showed the highest intensity compared to other groups. These observations suggest that carbofuran synergistically accelerated senescence activity in *spns1*^{-/-} mutant fish.

3.2 | Carbofuran exacerbates premature ageing phenotype and lifespan in *spns1*^{-/-} mutant zebrafish

Embryonic senescence has been implicated in the regulation of the ageing process. Accelerated senescence can trigger ageing symptoms and declines organismal longevity.^{5,14} A premature ageing phenotype in *spns1*^{-/-} mutant zebrafish is yolk opaqueness, which typically begins from the posterior end of yolk extension and gradually progresses towards other parts of yolk extension and yolk.^{14,15} If a small part of the yolk and/or yolk extension of the embryo becomes opaque, then it is denoted as a 'partially opaque.' On the other hand, when the major part of yolk and yolk extension become opaque, then it is denoted as 'mostly opaque' (Figure 2A).¹⁵ Mostly opaque embryos usually die within the subsequent 24-48 hours.

Heterozygous *spns1*^{+/-} adult fishes were incrossed, and resultant embryos were treated with low (10 μ mol/L) and high (100 μ mol/L) doses of carbofuran since 20 hpf. Treated embryos were monitored at each 12 hours intervals for yolk opaqueness phenotype and survival data. Among embryos of both control and carbofuran treated groups, around 25% have revealed yolk opaqueness phenotype (Figure 2B). Yolk opaqueness phenotype of embryos of low-dose carbofuran treatment group was almost similar to that of the control group. Almost all embryos of high-dose carbofuran treated group became mostly opaque at 48 hpf, whereas remarkable parts of embryos of both control and low-dose carbofuran treated groups remained partially opaque (Figure 2B), suggesting that carbofuran treatment (100 μ mol/L) exacerbated the premature ageing

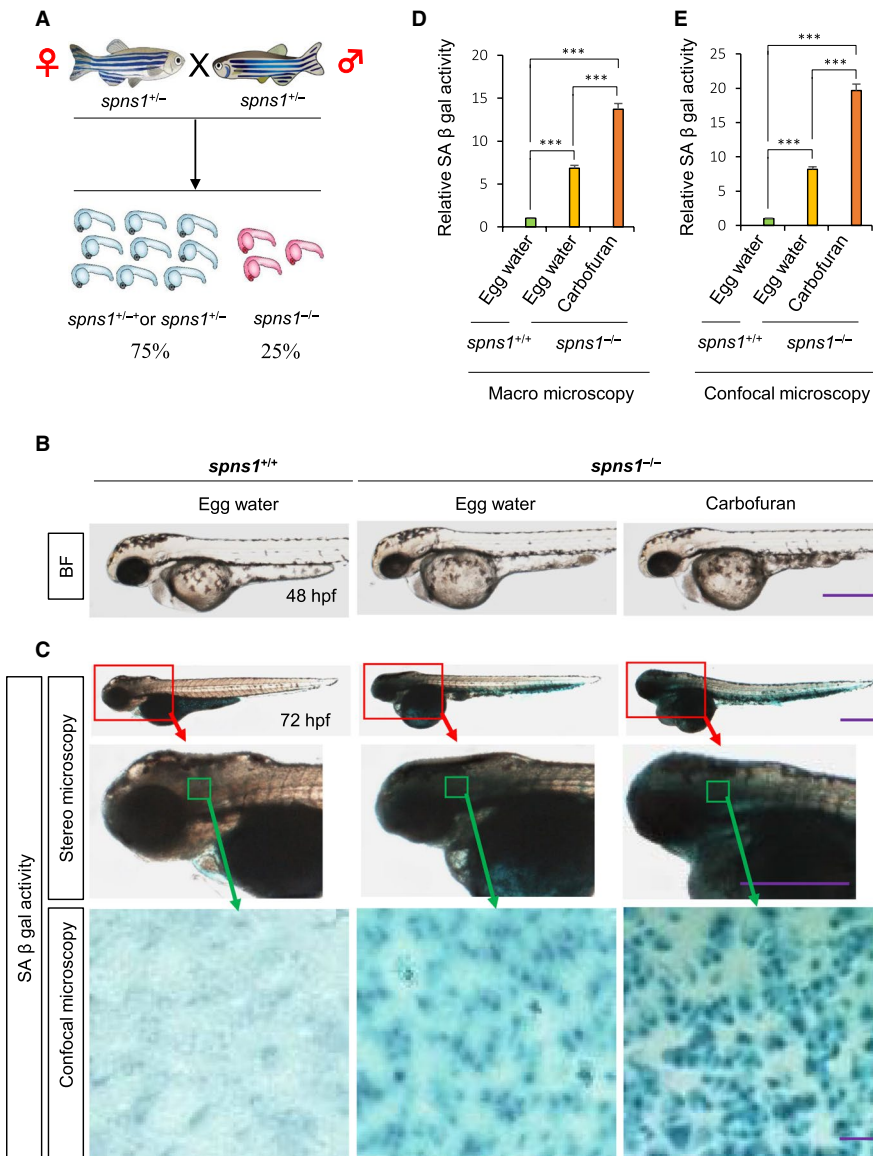


FIGURE 1 Carbofuran accelerated yolk opaqueness and SA-β-galactosidase activity in *spns1* mutant zebrafish. **A**, Incross among heterozygote (*spns1^{+/-}*) fishes. Around 25% of resultant embryos are *spns1^{-/-}* homozygous mutant, whereas the remaining 75% of embryos consist of wild (*spns1^{+/+}*) and heterozygous (*spns1^{+/-}*) embryos. **B**, Yolk opaqueness phenotype in homozygote (*spns1^{-/-}*) fish. The opaqueness was accelerated by carbofuran exposure. **C**, The SA-β-gal activity was high in homozygote (*spns1^{-/-}*) fish and accelerated by exposure to carbofuran. The SA-β-gal staining at the head was expanded, as shown by a red box and red arrow. The SA-β-gal staining of whole fish was observed under the bright field (BF) condition of the stereo-microscope. The cellular SA-β-gal staining in the head (shown by green box and arrow) was observed by confocal microscopy. The scale bars are 250 mm (stereo microscopic images) and 10 mm (confocal microscopic images). **D**, Quantification of SA-β-gal staining intensity of whole fish. **E**, Quantification of cellular SA-β-gal staining signals in the head region. The number of animals was 10 ($n = 10$). *** $P \leq .005$

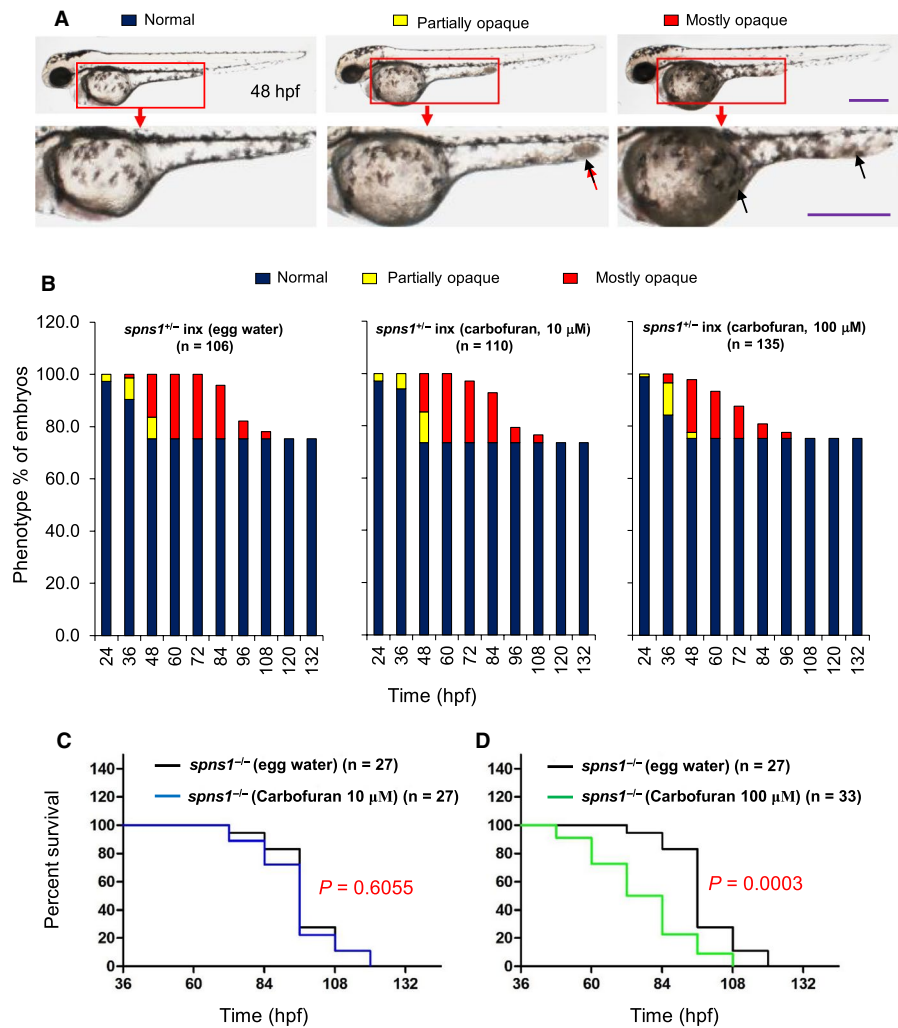
phenotype in *spns1^{-/-}* mutant fish. In addition, among embryos of the high-dose carbofuran treated group, mostly opaque embryos died at an earlier time than that observed in the case of embryos of other groups (Figure 2B). Kaplan-Meier survival analysis for *spns1^{-/-}* mutant larvae showed that the survival patterns of low-dose carbofuran (10 $\mu\text{mol/L}$) treated larvae were nearly similar to the survival patterns of larvae of the control group, whereas the survival of larvae treated with 100 $\mu\text{mol/L}$ of carbofuran was significantly shortened (Figure 2C).

3.3 | Carbofuran accelerates autophagy formation in *spns1^{-/-}* mutant zebrafish

Cellular autophagy is essential to maintain cellular homeostasis.¹¹ It has an advantageous effect on organismal longevity.¹² Under stress conditions of the body such as growth factor withdrawal, hypoxia, starvation, tumour progression and ageing, autophagy is

up-regulated above the normal baseline level.⁹ During autophagy, cytosolic microtubule-associated protein 1 light chain 3-II (LC3) associated autophagosomes are fused to lysosomes and subsequently sequestered by lysosomal enzymes.^{10,12} We have EGFP-tagged LC3 transgenic zebrafish on *spns1^{+/-}* (heterozygous) background. Mutant (*spns1^{-/-}*) embryos were treated with carbofuran since 40 hpf and subjected to lysosomal red staining before imaging. Excess autolysosome formation in *spns1^{-/-}* mutant fishes above normal limit was suggested by Sasaki et al.¹² Our current experiment reconfirmed his finding and additionally found carbofuran treatment synergistically accelerates autolysosome formation in *spns1^{-/-}* mutant fish. Both autophagosomal (represented by EGFP-tagged LC3) and lysosomal (represented by LysoTracker red) expressions were significantly increased in carbofuran treated *spns1^{-/-}* mutant fish in comparison to the fishes of other groups (Figure 3A-C). The co-localization of autophagosomal and lysosomal expressions was also found significant (merge images, yellow colour; Figure 3A,D), suggesting autophagosomes were fused with lysosomes to form autolysosomes. However,

FIGURE 2 Carbofuran exacerbated the *spns1* deficiency phenotype and shortened the survival of *spns1* mutant zebrafish. A, Sorts of yolk opaeness phenotypes in *spns1*^{-/-} (homozygous) zebrafish based on the extent of opacity in the yolk and/or yolk extension: partially opaque (yellow colour) and mostly opaque (red colour). Wild (*spns1*^{+/+}) and heterozygous (*spns1*^{+/-}) zebrafish do not show such opaeness (dark blue colour). B, Effect of carbofuran on the opaeness phenotype of *spns1* mutant fish and death record. The opaeness phenotype and death records were not affected by 10 $\mu\text{mol/L}$ carbofuran exposure. However, the mostly opaque phenotype and death of embryos of 100 $\mu\text{mol/L}$ carbofuran treated group were found at earlier times than fishes of the control group (egg water treatment). C, Survival curves of *spns1* mutant fishes for carbofuran treatment at 10 and 100 $\mu\text{mol/L}$ concentrations. By 100 $\mu\text{mol/L}$ carbofuran exposure, the survival of *spns1* mutant fishes was significantly declined ($P = .0003$)



because of insufficient lysosome-mediated degradation, the autolysosomes were accumulated in cells.

The lysosomal-associated membrane protein 1 (Lamp1) is a glycoprotein encoded by the *Lamp1* gene, widely used as a lysosomal membrane marker.³⁷ To further confirm the co-localization of autophagosomal expression to lysosomes, we used a double-transgenic *spns1*^{+/-} heterozygous fish, expressing EGFP-tagged LC3 and mCherry-tagged Lamp1. We found that both autophagosomal EGFP-LC3 and lysosomal mCherry-Lamp1 expressions were excessively aggregated in carbofuran treated *spns1*^{-/-} mutant fish compared to the fishes of other groups (Figure 4A-C). Co-localization of EGFP-LC3 vesicles to mCherry-Lamp1 vesicles was more significant in carbofuran treated *spns1*^{-/-} mutant fish than that found in the case of *spns1*^{-/-} mutant fish (Figure 4A,D). Furthermore, in *spns1*^{-/-} mutant fish, both autophagosomal and lysosomal vesicle sizes were increased and the increments were accelerated by the carbofuran treatment (Figures 3A and 4A). These results together suggest that the effect of carbofuran on the ageing of *spns1*^{-/-} mutant fish has mediated through its detrimental effect on the cellular autophagic process.

3.4 | Carbofuran affects ageing-associated genes regulation in *spns1*^{-/-} mutant zebrafish

The impact of carbofuran exposure on ageing-related genes regulations was examined by RT-PCR analysis. Plasminogen activator inhibitor-1 (*pai1*) is encoded in humans by the *SERPINE1* gene, whose up-regulation is a risk factor for atherosclerosis.³⁸ In elderly individuals, its level is elevated, which may lead to multiple pathologies such as vascular sclerosis, emotional stress, insulin resistance and obesity.³⁹ Another gene, *p21*, is a cyclin-dependent kinase inhibitor, promotes cellular senescence.⁴⁰ In both prematurely aged mice and normal aged mice, the *p21* level was found elevated.⁴¹ In our investigation, the expression levels of both *pai1* and *p21*mRNA were significantly up-regulated by carbofuran exposure to *spns1* mutant fish (Figure 5). On the other hand, senescence marker protein 30 (*Smp30*) is a calcium-binding protein, was first recognized as a down-regulated protein in elderly individuals.⁴² The expression of *smp30* was down-regulated by the carbofuran treatment to *spns1* mutant fish (Figure 5).

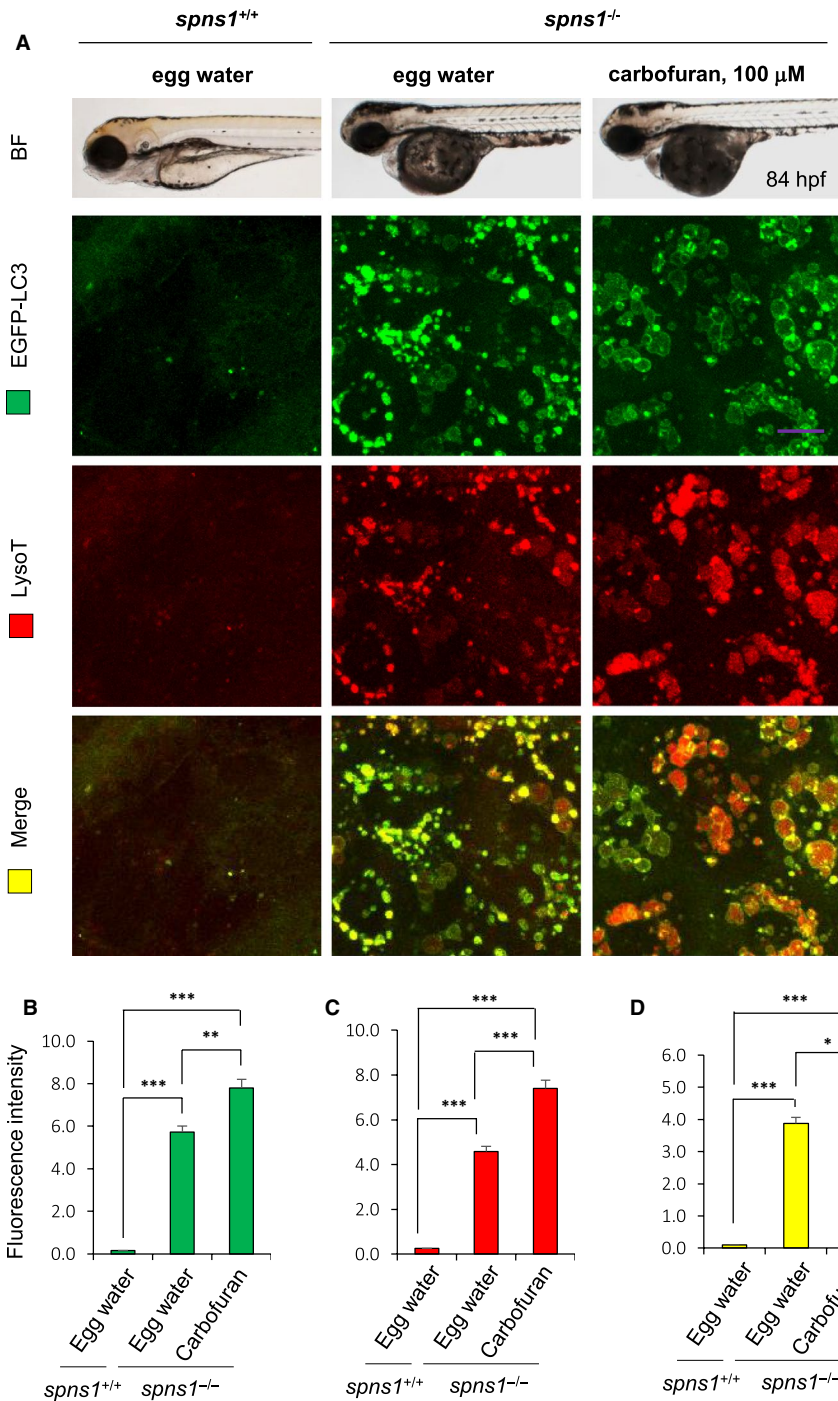


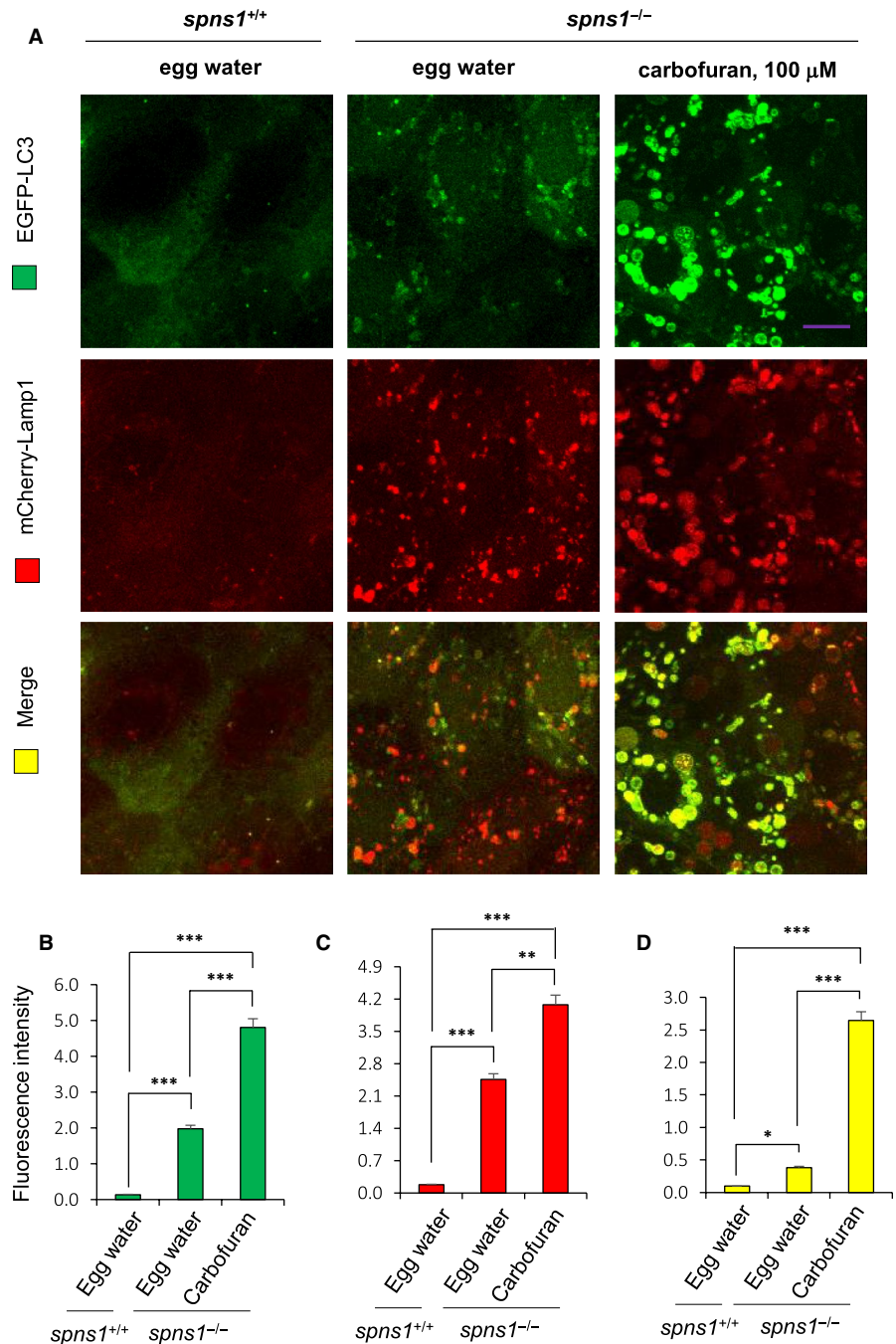
FIGURE 3 Carbofuran accelerated autolysosomal puncta formation in *spns1* mutant zebrafish. A, Carbofuran treatment worsened the yolk opaqueness phenotype of *spns1* mutant fishes, and most embryos lost their yolk extension. Loss of the *spns1* gene increased autophagosomal EGFP-LC3 and lysosomal LysoTracker (LysoT) red expressions, which were further accelerated by carbofuran exposure. Most LysoTracker red expressions were co-localized with EGFP-LC3 expressions (bottom row; yellow colour). B, Quantification of autophagosomal EGFP-LC3 expression. C, Quantification of LysoTracker red expression. D, Quantification of the merged expression (co-localization). These expressions were significantly increased by the loss of *spns1* gene and were further significantly up-regulated by carbofuran exposure. The scale bar is 10 μ m; n = 6; * $P \leq .05$; ** $P \leq .01$; *** $P \leq .005$

4 | DISCUSSION

Carbofuran is a broad-spectrum pesticide, which is non-specific in its action.⁴³ It also exerts its toxic effects on non-target animals, including fishes, beneficial arthropods and humans.⁴³⁻⁴⁵ In mammals, carbofuran exposure leads to oxidative stress, which in turn induces neuronal injury and neuronal cell death through the inhibition of acetylcholinesterase (AChE) activity.^{17,27} It was demonstrated that the inhibition of AChE by carbofuran is mediated by the carbamylation of the serine molecule of AChE.¹⁷ Although the toxicity of carbofuran is dose-dependent, it can induce oxidative stress in the brain

at sub-lethal doses.¹⁷ The major ROS species in the body are generated via a disorganized electron transfer process of the mitochondrial respiratory chain.⁴⁶ At a tolerable extent, ROS that generated in mitochondria may activate an adaptive defence mechanism to prevent unexpected outcome.⁴⁷ ROS by acting as nucleophilic compounds might cause epigenetic modification of DNA (such as DNA methylation, histone modification) that control genes transcription and expression.⁴⁸ The epigenetic machinery copes with the advanced homeostasis impairment, which reshapes the nervous, cardiovascular and respiratory systems in the elder individuals.⁴⁹ When the ROS level exceeds the tolerable extent, the developed

FIGURE 4 Carbofuran accelerated autolysosomal puncta formation in a double-transgenic zebrafish line of *spns1* mutant background, expressing EGFP-LC3 and mCherry-Lamp1. A, Carbofuran exposure accelerated both autophagosomal EGFP-LC3 and lysosomal mCherry-Lamp1 expressions in *spns1* mutant zebrafish. Lysosomal mCherry-Lamp1 expression was merged to EGFP-LC3 expression (bottom row; yellow colour). B, Quantification of autophagosomal EGFP-LC3 expression. C, Quantification of lysosomal mCherry-Lamp1 expression. D, Quantification of the co-localization of expressions. Both EGFP-LC3 and mCherry-Lamp1 expressions (with their co-localization) were significantly increased by the loss of the *spns1* gene and were further significantly up-regulated by carbofuran exposure. The scale bar is 10 mm; $n = 6$; * $P \leq .05$; ** $P \leq .01$; *** $P \leq .005$



adaptive responses become insufficient, which leads to cellular stress.^{50,51} ROS dependent cellular stress accelerates the ageing process through the induction of cellular senescence.⁴⁷ Oxidative stress and cellular senescence are highly linked to ageing-related pathologies such as neurodegenerative diseases, diabetes, hypertension and atherosclerosis.⁵² A premature ageing phenotype in zebrafish is the yolk opaqueness, which was worsened by carbofuran treatment in *spns1*^{-/-} mutant zebrafish. However, the yolk and/or yolk extension was not affected by carbofuran treatment in wild zebrafish (Figure S1). The SA β -gal activity was weakly affected in wild zebrafish but synergistically accelerated by the carbofuran treatment in *spns1*^{-/-} mutant fish (Figure 1C, Figure S1). Furthermore, the life span of *spns1*^{-/-} mutant fish was shortened by carbofuran

exposure. These senescence and ageing effects of carbofuran in *spns1*^{-/-} mutant fish might be mediated by carbofuran-induced ROS generation (Figure 6), because elevated ROS level is a key factor of ageing-related pathologies such as neurodegenerative diseases, endocrine abnormalities and reproductive impairments.^{25,29} The loss of the *spns1* gene in the mutant zebrafish induces genotoxic stress, which was revealed by yolk opaqueness, senescence and shortened life span.^{14,34} Carbofuran-induced ROS generation made additional stress in *spns1* mutant fish and exacerbated these phenotypes of the *spns1* deficiency. In the senescent cell, oxidative stress affects epigenetic machinery via DNA hypomethylation, which is considered a representative phenotype of the ageing process. In cells of an elderly individual, such as leucocytes of females of around 100 years old,

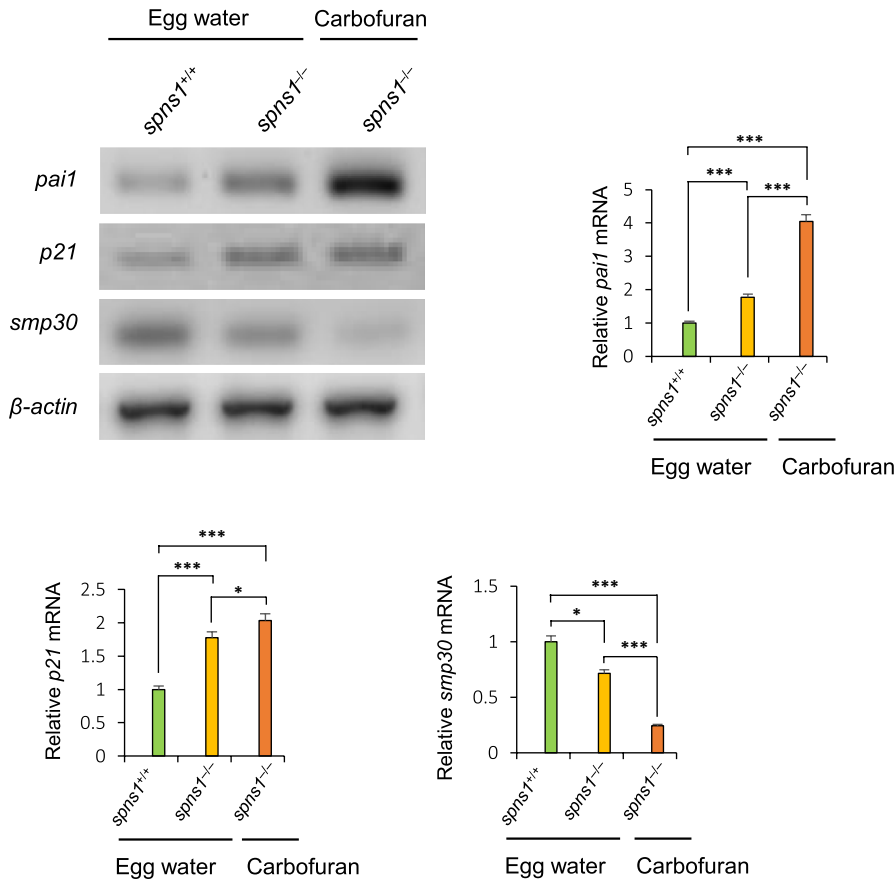


FIGURE 5 RT-PCR analysis to determine the effect of carbofuran on *pai1*, *p21* and *smp30* mRNA levels. The expressions levels of *pai1* and *p21* were increased by the loss of the *spns1* gene. Carbofuran treatment further increased their expressions. The expression of *smp30* was significantly down-regulated by carbofuran exposure in *spns1* mutant zebrafish. $n = 5$; $*P \leq .05$; $***P \leq .005$

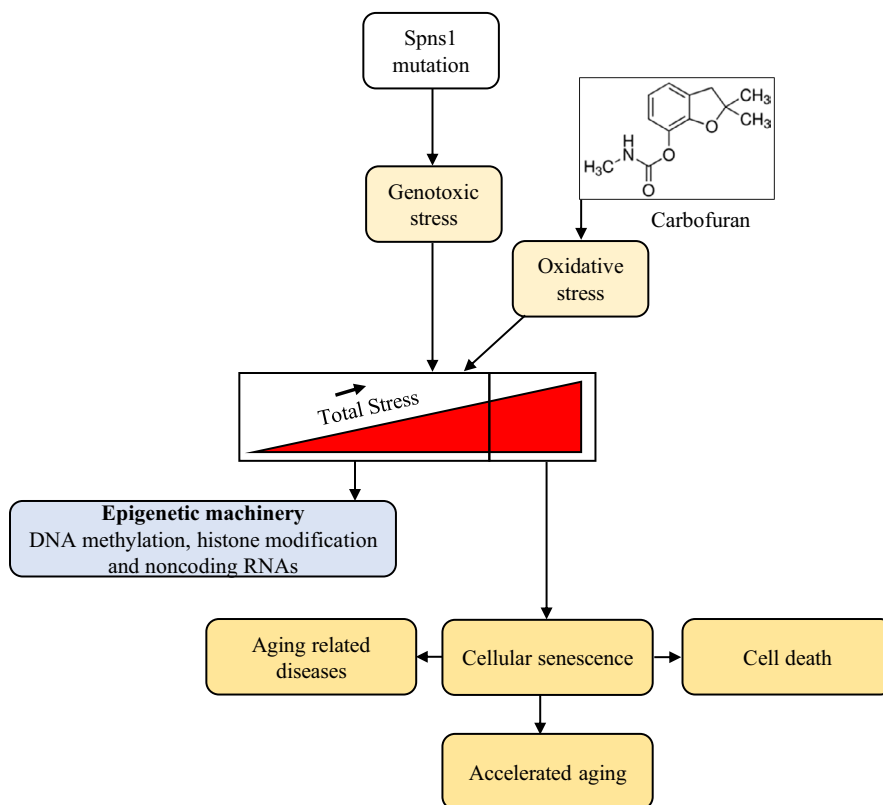


FIGURE 6 A proposed schematic model for the senescence and ageing effect of carbofuran under *spns1* defective condition. Cellular untoward events are prevented at low to medium stress conditions by epigenetic adjustment. The *Spns1* defect via strong genotoxic stress induces untoward events, such as senescence, ageing, ageing-related diseases and cell death. Carbofuran-induced oxidative stress accelerates these untoward cellular events in *spns1* defective animals

age-associated reduction of DNA methylation was manifested.⁴⁸ In senescent cells of the *spns1* defective fish, carbofuran-induced oxidative stress might affect the ageing process through DNA hypomethylation.

Senescence is elicited by autophagic commencement.¹² At the beginning of autophagy, phagophore is evolved in autophagosome through the elongation of the membrane of the phagophore. During the elongation process, an ubiquitin-like molecule LC3 is conjugated to phosphatidylethanolamine at the membrane of the autophagosome, leading to the formation of autophagosome-associated LC3.^{53,54} LC3 exists with autophagosomes until autolysosomal fusion and then delipidated and recycled.⁵³ In our in vivo real-time monitoring of EGFP-tagged LC3 protein on *spns1* mutant context, carbofuran accelerated LC3 puncta accumulation at the same pattern as we detected the acceleration of senescence induction using SA- β gal staining, suggesting carbofuran-induced autophagic abnormality is associated with accelerated senescence. It was demonstrated that autophagy is usually up-regulated by oxidative stress including cellular senescence,⁸ which is consistent with our findings.

Cellular intralysosomal waste materials are collectively known as lipofuscin, whose principal constituents are protein and lipid, and other constituents include carbohydrate, autofluorescent pigment and transition metals.⁵⁵ The lipofuscin accumulates in several cell types (such as neurons and cardiac cells) of aged individuals. It was demonstrated that lipofuscin accumulation is associated with lysosomal dysfunction.⁵⁶ The accumulation further increases in an ageing allied neurodegenerative disorder such as Alzheimer's disease.⁵⁶ Under oxidative stress conditions, increased autophagosome formation leads to the delivery of undegradable oxidized protein to the lysosome that accumulates as lipofuscin.⁵⁶ Using LysoTracker red staining and mCherry-tagged Lamp1 expression in *spns1* deficit fish, we found excessive lysosomal expression, which was further increased by carbofuran exposure. This lysosomal overexpression upon carbofuran exposure might be because of lipofuscin accumulation under stress conditions, which need further studies to explore the mode of lipofuscinogenesis implicated with carbofuran exposure. In addition, lysosome was significantly co-localized with autophagosome, suggesting successful autolysosomal fusion with insufficient lysosome facilitated degradation of the content of autophagosome. Such lysosomal dysfunction also validated under the *spns1* deficit stress condition.¹⁵ Some compounds such as chloroquine through oxidative stress and lipofuscin accumulation inhibit lysosomal proteases.^{56,57} A decline in lysosomal degradation in carbofuran treated zebrafish might also be because of the inhibition of the lysosomal proteases, but it needs further studies to be confirmed. Overall, carbofuran exacerbated lysosomal dysfunction in *spns1* deficit fish.

The effects of carbofuran on developmental senescence and biological ageing are consistent with its effects on ageing allied genes regulation in *spns1*^{-/-} mutant fish. It was demonstrated that the inhibition of the *pai1* gene down-regulates SA- β -gal activity,⁵⁸ whereas, in our investigation, SA- β -gal activity was concurrently increased with the *pai1* mRNA level. An increment in the *pai1* expression is associated with ageing and age-related multimorbidity

such as cognitive dysfunction, hypertension, atherosclerosis and glucose intolerance,^{58,59} whereas we consistently found that carbofuran exposure shortened the life span of *spns1* mutant fish. A potent cyclin-dependent kinase inhibitor, *p21*, whose up-regulation is maintained in senescent cells. The intensity of senescence cells was decreased with the loss of the *p21* gene in mice.⁴⁰ The up-regulation of *p21* arrest cellular proliferation and promote age-associated pathologies.⁶⁰ It was also reported that the level of *p21* in the neuronal cells of rats was up-regulated by carbofuran treatment.²⁹ Constantly, an elevation of the *p21* mRNA level in *spns1* mutant zebrafish was observed in our investigation. On the other hand, *smg30* is a calcium homeostasis gene, protects apoptosis and prevents oxidative stress by reducing ROS generation.⁶⁰ Carbofuran exposure to *spns1* mutant fish down-regulated the expression of *smg30*, which might be because of additional oxidative stress in *spns1* mutant fish. Altogether, our data suggest that carbofuran accelerated cellular senescence and shortened biological ageing in *spns1* mutant zebrafish through autophagic dysregulation.

ACKNOWLEDGEMENTS

The works of this manuscript mainly supported by The World Academy of Science (TWAS) fund (grant No. 17-414 RG/BIO/AS_I - FR3240297760) and partly by Rajshahi University Research grant (grant No. A1386/5/52/RU/Science-24/18-19) and Ministry of Science and Technology Special Allocation Research Fund (grant No. 39.00.0000.009.06.024.19-665/460-ID).

CONFLICT OF INTEREST

The authors of this manuscript have no conflicts of interest.

AUTHOR CONTRIBUTIONS

Alam Khan: Conceptualization (lead); Data curation (supporting); Methodology (lead); Writing-review & editing (lead). **T M Fahad:** Data curation (lead); Formal analysis (lead); Investigation (lead). **Tanjima Akther:** Data curation (lead); Formal analysis (lead); Investigation (lead); Writing-original draft (equal). **Tanjeena Zaman:** Investigation (equal); Methodology (equal); Project administration (equal). **Md Faruk Hasan:** Investigation (equal); Writing-review & editing (equal). **Md Rafiqul Islam:** Investigation (equal). **Mohammad Saiful Islam:** Data curation (equal); Formal analysis (lead). **Shuji Kishi:** Conceptualization (lead); Writing-review & editing (equal).

DATA AVAILABILITY STATEMENT

The data that support the findings of this study are available from the corresponding author upon reasonable request.

ORCID

Alam Khan  <https://orcid.org/0000-0002-2482-7403>

REFERENCES

1. Rhinn M, Ritschka B, Keyes WM. Cellular senescence in development, regeneration and disease. *Development*. 2019;146(20):151837.

2. Barbouti A, Vasileiou PVS, Evangelou K, et al. Implications of oxidative stress and cellular senescence in age-related thymus involution. *Oxid Med Cell Longev*. 2020;2020:7986071.
3. Pawlowska E, Szczepanska J, Szatkowska M, Blasiak J. An interplay between senescence, apoptosis and autophagy in glioblastoma multiforme-role in pathogenesis and therapeutic perspective. *Int J Mol Sci*. 2018;19(3):889.
4. Storer M, Mas A, Robert-Moreno A, et al. Senescence is a developmental mechanism that contributes to embryonic growth and patterning. *Cell*. 2013;155(5):1119-1130.
5. Koshimizu E, Imamura S, Qi J, et al. Embryonic senescence and laminopathies in a progeroid zebrafish model. *PLoS One*. 2011;6(3):e17688.
6. Kurz DJ, Decary S, Hong Y, Erusalimsky JD. Senescence-associated (beta)-galactosidase reflects an increase in lysosomal mass during replicative ageing of human endothelial cells. *J Cell Sci*. 2000;113:3613-3622.
7. Boya P, Reggiori F, Codogno P. Emerging regulation and functions of autophagy. *Nat Cell Biol*. 2013;15:713-720.
8. Kang C, Elledge SJ. How autophagy both activates and inhibits cellular senescence. *Autophagy*. 2016;12(5):898-899.
9. Huang J, Lam GY, Brumell JH. Autophagy signaling through reactive oxygen species. *Antioxid Redox Signal*. 2011;14:2215-2231.
10. Tanida I. Autophagosome formation and molecular mechanism of autophagy. *Antioxid Redox Signal*. 2011;14:2201-2214.
11. Mauvezin C, Nagy P, Juhasz G, Neufeld TP. Autophagosome-lysosome fusion is independent of V-ATPase-mediated acidification. *Nat Commun*. 2015;6:7007.
12. Sasaki T, Lian S, Qi J, et al. Aberrant autolysosomal regulation is linked to the induction of embryonic senescence: differential roles of Beclin 1 and p53 in vertebrate Spns1 deficiency. *PLoS Genet*. 2014;10(6):e1004409.
13. Rong Y, McPhee CK, Deng S, et al. Spinster is required for autophagic lysosome reformation and mTOR reactivation following starvation. *Proc Natl Acad Sci*. 2011;108(19):7826-7831.
14. Kishi S, Bayliss PE, Uchiyama J, et al. The identification of zebrafish mutants showing alterations in senescence-associated biomarkers. *PLoS Genet*. 2008;4(8):e1000152.
15. Sasaki T, Lian S, Khan A, Chen W, Klionsky DJ, Kishi S. Spatiotemporal counteraction between the defects of Spns1 and v-ATPase in premature autolysosomal fusion and developmental senescence. *Autophagy*. 2017;13(2):386-403.
16. Singh RK, Sharma B. Carbofuran induced biochemical changes in *Clarias batrachus*. *Pestic Sci*. 1998;53:285-290.
17. Jaiswal SK, Sharma A, Gupta VK, Singh RK, Sharma B. Curcumin mediated attenuation of carbofuran induced oxidative stress in rat brain. *Biochem Res Int*. 2016;2016:7637931.
18. Seth B, Yadav A, Tandon A, Shankar J, Chaturvedi RK. Carbofuran hampers oligodendrocytes development leading to impaired myelination in the hippocampus of rat brain. *Neurotoxicology*. 2019;70:161-179.
19. Sharma RK, Jaiswal SK, Siddiqi NJ, Sharma B. Effect of carbofuran on some biochemical indices of human erythrocytes *in vitro*. *Cell Mol Biol (Noisy-le-grand)*. 2012;58:103-109.
20. Jaiswal SK, Gupta VK, Ansari MD, Siddiqi NJ, Sharma B. Vitamin C acts as a hepatoprotectant in carbofuran treated rat liver slices *in vitro*. *Toxicol Rep*. 2017;4:265-273.
21. Kabir KH, Abdullah M, Prodhann MDH, Ahmed MS, Alam MS. Determination of carbofuran residue in the samples of sugarcane (*sacharum officinarum* L) and soil of sugarcane field. *Agriculturists*. 2007;5(1,2):61-66.
22. Rai DK, Sharma B. Carbofuran induced oxidative stress in mammalian brain. *Mol Biotechnol*. 2007;37(1):66-71.
23. Sharma RK, Sharma B. *In-vitro* carbofuran induced genotoxicity in human lymphocytes and its mitigation by vitamins C and E. *Dis Markers*. 2012;32:153-163.
24. Gammon DW, Liu Z, Becker JM. Carbofuran occupational dermal toxicity, exposure and risk assessment. *Pest Manag Sci*. 2012;68:362-370.
25. Jaiswal SK, Siddiqi NJ, Sharma B. Carbofuran induced oxidative stress mediated alterations in Na(+)-K(+)-ATPase activity in rat brain: amelioration by vitamin E. *J Biochem Mol Toxicol*. 2014;28(7):320-327.
26. Rai DK, Rai PK, Rizvi SI, Watal G, Sharma B. Carbofuran induced toxicity in rats: protective role of vitamin C. *Exp Toxicologic Pathol*. 2009;61(6):531-535.
27. Gupta RC, Milatovic S, Dettbarn WD, Aschner M, Milatovic D. Neuronal oxidative injury and dendritic damage induced by carbofuran: protection by memantine. *Toxicol Appl Pharmacol*. 2007;219(2-3):97-105.
28. Chen NN, Luo DJ, Yao XQ, et al. Pesticides induce spatial memory deficits with synaptic impairments and an imbalanced tau phosphorylation in rats. *J Alzheimers Dis*. 2012;30(3):585-594.
29. Seth B, Yadav A, Agarwal S, Tiwari SK, Chaturvedi RK. Inhibition of the transforming growth factor- β /SMAD cascade mitigates the anti-neurogenic effects of the carbamate pesticide carbofuran. *J Biol Chem*. 2017;292(47):19423-19440.
30. Jaiswal SK, Siddiqi NJ, Sharma B. Studies on the ameliorative effect of curcumin on carbofuran induced perturbations in the activity of lactate dehydrogenase in wistar rats. *Saudi J Biol Sci*. 2018;25:1585-1592.
31. Kimmel CB, Ballard WW, Kimmel SR, Ullmann B, Schilling TF. Stages of embryonic development of the zebrafish. *Dev Dyn*. 1995;203:253-310.
32. He C, Bartholomew CR, Zhou W, Klionsky DJ. Assaying autophagic activity in transgenic GFP-Lc3 and GFP-Gabarap zebrafish embryos. *Autophagy*. 2009;5(4):520-526.
33. Debaq-Chainiaux F, Erusalimsky JD, Campisi J, Toussaint O. Protocols to detect senescence-associated beta-galactosidase (SA- β gal) activity, a biomarker of senescent cells in culture and *in vivo*. *Nat Protoc*. 2009;4:1798-1806.
34. Young RM, Marty S, Nakano Y, et al. Zebrafish yolk-specific *not really started (nrs)* gene is a vertebrate homolog of the *Drosophila spinster* gene and is essential for embryogenesis. *Dev Dyn*. 2002;223(2):298-305.
35. Wang JH, Ahn IS, Fischer TD, et al. Autophagy suppresses age-dependent ischemia and reperfusion injury in livers of mice. *Gastroenterology*. 2011;141:2188-2199.
36. He C, Klionsky DJ. Analyzing autophagy in zebrafish. *Autophagy*. 2010;6:642-644.
37. Agarwal AK, Srinivasan N, Godbole R, et al. Role of tumor cell surface lysosome-associated membrane protein-1 (LAMP1) and its associated carbohydrates in lung metastasis. *J Cancer Res Clin Oncol*. 2015;141:1563-1574.
38. Vaughan DE. PAI-1 and atherothrombosis. *J Thromb Haemost*. 2005;3(8):1879-1883.
39. Yamamoto K, Takeshita K, Kojima T, Takamatsu J, Saito H. Aging and plasminogen activator inhibitor-1 (PAI-1) regulation: implication in the pathogenesis of thrombotic disorders in the elderly. *Cardiovasc Res*. 2005;66:276-285.
40. Papismadov N, Gal H, Krizhanovsky V. The anti-aging promise of p21. *Cell Cycle*. 2017;16:1997-1998.
41. Edwards MG, Anderson RM, Yuan M, Kendziorski CM, Weindruch R, Prolla TA. Gene expression profiling of aging reveals activation of a p53-mediated transcriptional program. *BMC Genom*. 2007;8:80.
42. Li S, Chen X, Lai W, et al. Down regulation of SMP30 in senescent human lens epithelial cells. *Mol Med Rep*. 2017;16:4022-4028.
43. Sharma RK, Rai DK, Sharma B. *In-vitro* carbofuran induced micronucleus formation in human blood lymphocytes. *Cell Mol Biol (Noisy-le-grand)*. 2012;58(1):128-133.

44. Singh RK, Singh RL, Sharma B. Acute toxicity of carbofuran to a freshwater teleost. *Clarias batrachus*. *Bull Environ Contam Toxicol*. 2003;70(6):1259-1263.
45. Singh RK, Sharma B. *In vivo* alteration in protein metabolism by sub-acute carbofuran intoxication in the freshwater teleost, *Clarias batrachus*. *Bull Environ Contam Toxicol*. 2004;73(5):919-926.
46. Davalli P, Mitic T, Caporali A, Lauriola A, D'Arca D. ROS, cell senescence, and novel molecular mechanisms in aging and age-related diseases. *Oxid Med*. 2016;2016:3565127.
47. Campisi J, Robert L. Cell senescence: role in aging and age-related diseases. *Interdiscipl Top Gerontol*. 2014;39:45-61.
48. Afanas'ev I. New nucleophilic mechanisms of ROS-dependent epigenetic modifications: comparison of aging and cancer. *Aging Dis*. 2014;5(1):52-62.
49. Cencioni C, Spallotta F, Martelli F, et al. Oxidative stress and epigenetic regulation in ageing and age-related diseases. *Int J Mol Sci*. 2013;14(9):17643-17663.
50. Genova ML, Lenaz G. The interplay between respiratory supercomplexes and ROS in aging. *Antioxid Redox Signal*. 2015;23(3):208-238.
51. Yan LJ. Positive oxidative stress in aging and aging-related disease tolerance. *Redox Biol*. 2014;2:165-169.
52. Liguori I, Russo G, Curcio F, et al. Oxidative stress, aging, and diseases. *Clin Interv Aging*. 2018;13:757-772.
53. Rubinsztein DC, Shpilka T, Elazar Z. Mechanisms of autophagosome biogenesis. *Curr Biol*. 2012;22:R29-R34.
54. Shpilka T, Weidberg H, Pietrokovski S, Elazar Z. Atg8: an autophagy-related ubiquitin-like protein family. *Genome Biol*. 2011;12:226.
55. Brunk UT, Jones CB, Sohal RS. A novel hypothesis of lipofuscinogenesis and cellular aging based on interactions between oxidative stress and autophagocytosis. *Mutat Res*. 1992;275:395-403.
56. Pivtoraiko VN, Stone SL, Roth KA, Shacka JJ. Oxidative stress and autophagy in the regulation of lysosome-dependent neuron death. *Antioxid Redox Signal*. 2009;11(3):481-496.
57. Hamano T, Gendron TF, Causevic E, et al. Autophagic-lysosomal perturbation enhances tau aggregation in transfectants with induced wild-type tau expression. *Eur J Neurosci*. 2008;27(5):1119-1130.
58. Sun T, Ghosh AK, Eren M, Miyata T, Vaughan DE. PAI-1 contributes to homocysteine-induced cellular senescence. *Cell Signal*. 2019;64:109394.
59. Wang L, Chen L, Liu Z, et al. PAI-1 exacerbates white adipose tissue dysfunction and metabolic dysregulation in high fat diet-induced obesity. *Front Pharmacol*. 2018;9:1087.
60. Yosef R, Pilpel N, Papismadov N, et al. p21 maintains senescent cell viability under persistent DNA damage response by restraining JNK and caspase signaling. *Embo J*. 2017;36(15):2280-2295.

SUPPORTING INFORMATION

Additional supporting information may be found online in the Supporting Information section.

How to cite this article: Khan A, Fahad TM, Akther T, et al. Carbofuran accelerates the cellular senescence and declines the life span of *spns1* mutant zebrafish. *J Cell Mol Med*. 2021;25:1048-1059. <https://doi.org/10.1111/jcmm.16171>